

Hydrogeochemical Processes Regulating the Groundwater Quality and its Suitability for Drinking and Irrigation Purpose in Parts of Coastal Sindhudurg District, Maharashtra

Suneetha Naidu^a, Gautam Gupta^{a,*}, Rambabu Singh^b, Khan Tahama^a and Vinit C. Erram^c

^aIndian Institute of Geomagnetism, New Panvel (W), Navi Mumbai - 410 218, India

^bExploration Department, Central Mine Planning and Design Institute Limited, Bilaspur - 495 006, India

^cMF Radar Facility, Indian Institute of Geomagnetism, Shivaji University Campus, Kolhapur - 416 004, India

*E-mail: gupta_gautam1966@yahoo.co.in

ABSTRACT

The hydrochemistry of groundwater samples from the northern part of coastal Sindhudurg district, Maharashtra, India, was studied with an aim to comprehend its suitability for domestic and irrigation use. Groundwater samples were collected from 66 dug wells distributed over the study area, during the month of November 2017. The results of the chemical analysis indicate that the groundwater is alkaline in nature and are mainly characterized by $\text{Ca}^+\text{-Mg}^{2+}\text{-HCO}_3^-$, $\text{Ca}^+\text{-Mg}^{2+}\text{-Cl}^-$ and $\text{Na}^+\text{-Cl}^-$ facies. The molar ratios of $\text{Na}^+/\text{Cl}^- > 1$, both $\text{Mg}^{2+}/\text{Na}^+$ and $\text{Ca}^{2+}/\text{Na}^+$ ratios < 1 , $(\text{Ca}^{2+} + \text{Mg}^{2+})/(\text{SO}_4^{2-} + \text{HCO}_3^-) = 1$ suggest that the rock-water interaction of silicates / schistose rocks (quartz, chlorite, amphibolites, schist etc.) and ion exchange reaction are the major controlling factors of groundwater chemistry. Lower molar ratios of $\text{Cl}^-/\text{HCO}_3^- < 0.5$, $\text{NO}_3^-/\text{Cl}^- < 0.3$ observed reflect freshwater regime. Three samples which are in proximity to the Arabian Sea, deduce the effect of secondary contributions (saline water and anthropogenic sources). In order to determine the probable sources of groundwater contamination, principal component analysis was also carried out. The first three principal components with eigen value 1 or more are responsible for 71.31 %, 12.38% and 8.32% of the total variance in the data set, indicating major role of groundwater-rock interaction and marginal saltwater intrusion effect in the study area. Groundwater quality index computed for drinking purpose indicate that about 96% of the water samples lie within the permissible limits stipulated by the World Health Organization and Bureau of Indian Standards, and fall under the good to excellent category, suggesting its suitability for drinking purpose in the area. Water quality index indicates that most of the water is of excellent to good quality for irrigation, except for a few coastal samples.

INTRODUCTION

Coastal aquifers are increasingly exploited throughout the world to meet water demand. Seawater has been observed in several coastal areas of the world (Werner and Simmons, 2008), and is more dominant when the natural balance between fresh and seawater is disturbed, resulting in deterioration of fresh water resources (Xue et al., 1999). In India the majority of the population is dependent on groundwater resources for drinking and domestic, industrial, and irrigation uses (Singha et al., 2019a,b). The alarming rate of population growth, improvements in technology, and the prevailing trend of depletion of groundwater resource has raised some severe environmental problems (Kumar et al., 2019; Naladala et al., 2019). The quality of drinking water has increasingly been questioned from

health point of view for several decades (Garget et al., 2009; Singh et al., 2018).

Therefore, information on hydrochemistry of freshwater is significant to evaluate the quality of groundwater, especially in coastal areas which influences the suitability of groundwater for domestic, irrigation, and industrial needs. The water quality may yield information about the environment through which the water has circulated. Environmental problems associated with groundwater vary from place to place and depend on the geology, hydrologic and climatic conditions, and geochemical factors. The contamination of water not only affects its quality but also threatens human health, economic development and social prosperity (Milovanovic, 2007; Naladala et al., 2018). Groundwater quality studies with reference to drinking and irrigation purposes in different regions worldwide have been carried out by many researchers (Rivers et al., 1996; Kalpana and Elango, 2013; Singh et al., 2017a). Further, it is important to understand how water-rock interaction (weathering) or any type of anthropogenic activities impact the degradation of groundwater quality (Todd, 1980; Singh et al., 2017b).

The area under study is the northern part of Sindhudurg district of coastal Maharashtra, India. Here, the groundwater is used for domestic, agricultural and industrial purposes. Being a coastal region, seawater intrusion is a serious concern for contamination of groundwater, apart from anthropogenic activities. Therefore, it is essential to undertake regular groundwater monitoring to focus on the groundwater quality in these growing urbanized environments. Moreover, no systematic water quality studies have been undertaken in this area so far. It is thus pertinent to note that such a study will not only provide a relationship between groundwater quality and human health but also aid the water managers to develop robust management strategies to improve groundwater quality in such hard rock terrains.

Thus the objective of the present study is four-fold, (i) to assess the physico-chemical parameters of groundwater, (ii) to examine the major ion chemistry so as to understand the hydrogeochemical processes taking place, which has a bearing on the groundwater quality, (iii) to establish the factors controlling the water chemistry, and (iv) to identify the areas where groundwater is suitable for drinking and agricultural purpose.

GEOLOGY AND HYDROGEOLOGY OF THE STUDY AREA

The Konkan coast is a narrow stretch of land located between the Arabian Sea to the west and the Sahyadri mountain range to its east in Maharashtra (Kumaran et al., 2004). The study area lies between latitude 16-16.5°N and longitude 73.3-73.73°E in Sindhudurg district of Maharashtra, India (Fig. 1). The climate in the district is influenced

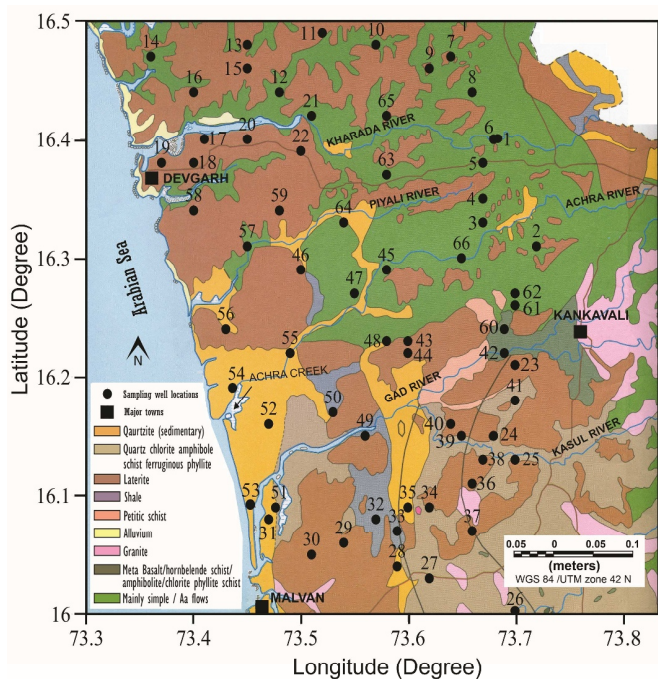


Fig.1. Map of the study area showing geology and the well location points.

by its geographical conditions, and fall under the 'Assured and High Rainfall zone'. The cold season is from December to February with mean daily maximum temperature at 32.7°C and the mean daily minimum temperature at 18.7°C, followed by summer from March to May. The southwest monsoon is dominant during June to September. Relative humidity ranging from 86% to 90% is recorded during the southwest monsoon, whereas during winter and summer months it is about 57% (Paranjape, 2009). The annual average rainfall is about 3287 mm over the Sindhudurg district. While the western part of the district along the coastal zone experiences minimum annual rainfall, it progressively increases towards east and reaches maximum along Western Ghats, Maharashtra.

The geographical area of the Sindhudurg district is 5207 km², of these about 386.43 km² is covered by forest, while the cultivable area is 3222 km² and net sown area is 1522 km² (CGWB, 2014). The study region reveals a typical physiographic setting having undulating terrain in the central part with elevations up to about 300 m above mean sea level (msl). These are flat-topped hills covered by laterites, while the western stretch comprises the coastal plain. The drainage pattern is dendritic in nature with high drainage density. The steep slopes and high drainage density contribute to the major runoff and thus little groundwater recharge. On the contrary, in the plain and valley areas where drainage density is low, recharge is generally good (Dikshit, 2001).

Geologically, the study area comprises of rocks in the range of Archean to Quaternary period. Dharwarian meta-sediments (Archean), Kaladgi Formation (Precambrian), Deccan Trap lava flows (Upper Cretaceous to Lower Eocene), laterites (Pleistocene) and alluvial deposits (Recent to sub-recent) are the water bearing formations observed in Sindhudurg district. However, the Kaladgi Formation occurs only in very restricted patches and thus does not form potential aquifers. The alluvium also occurs in limited area, found mainly along the coast (CGWB, 2014). Laterite has more porosity than the Deccan Trap basalt, thereby forming many potential aquifers in the area. Groundwater level in the study area varies from 2 m to 20 m below ground level (bgl) (Maiti et al., 2012). Shallow water levels within 10 m bgl are reported in almost entire district during pre-monsoon season.

The deeper water levels varying from 10-20 m bgl are observed in north western part of the district. Spatial variation of water levels is about 5 m bgl in the entire district during post-monsoon season (CGWB, 2014). Agriculture is the primary occupation of the district and major crops grown are rice, coconut, kokam, mango and cashew.

MATERIALS AND METHODOLOGY

Sampling and Analysis

A total of 66 water samples (Fig. 1) were collected during the post-monsoon period (November 2017) from dug wells at 0.5 m below groundwater level in 1000 mL plastic bottles. Before the collection of water samples, the bottles were pre-rinsed thoroughly with diluted HCl acid and then rinsed with the water from the sampling location. The bottles were filled with water from the dug wells and sealed with double plastic caps so as to avoid evaporation. The water samples collected in the field were analysed for pH, electrical conductivity (EC), total dissolved solids (TDS), total hardness (TH), calcium (Ca²⁺), magnesium (Mg²⁺), sodium (Na⁺), potassium (K⁺), bicarbonate (HCO₃⁻), chloride (Cl⁻), sulphate (SO₄²⁻), nitrate (NO₃⁻) and fluoride (F⁻), following the standard water quality procedures (APHA, 2012). The flow chart of the methodology adopted for groundwater quality is presented in Fig. 2. Ca²⁺, Mg²⁺, HCO₃⁻, CO₃²⁻, and Cl⁻ were analyzed by volumetric titration method. The flame photometer technique was used to measure the concentration of Na⁺ and K⁺ ions. SO₄²⁻, NO₃⁻, and F⁻ ions were determined by spectrophotometric technique.

In order to check the reliability of the water quality data for major ionic species distinctively, the percent of error in cation-anion, ionic balance error (IBE) technique was performed (Freeze and Cherry, 1979). In this scheme, the sum of the positive ions (cations) must equal the sum of the negative ions (anions). The IBE should be less than ±5% for good measurement and if it is greater than ± 5%, the analysis is supposed to be poor (Hounslow, 1995). The electrical imbalance of cations-anions could be due to instrumental/analytical errors or some dissolved species wherein major ions which are present in the samples are not measured. The error percentage in cation-anion balance (IBE) was computed by the following equation after Hem (1991); Freeze and Cherry (1979).

$$IBE = \frac{\sum cations - \sum anions}{\sum cations + \sum anions} \times 100$$

All concentrations are expressed in meq/L.

In the present case, all the samples are within good measurement limit except two samples which are above detection limit. The

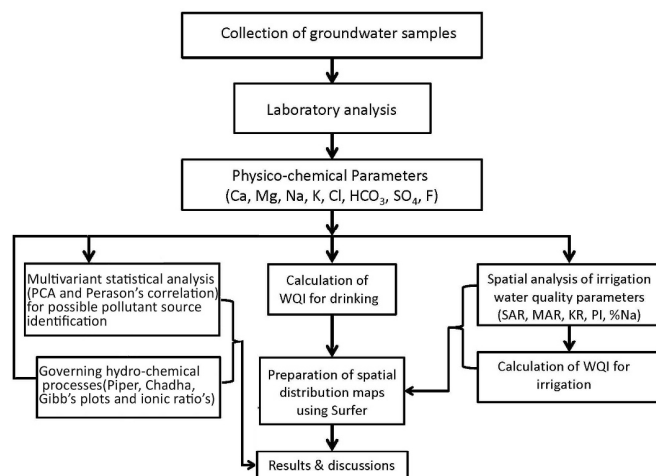


Fig.2. Flowchart of the methodology for groundwater quality.

correlation between total sum of cations and anions indicate that there is a fair degree of linear correlation.

Piper trilinear diagrams were plotted using Aquachem 3.7 software package, while Chadha's diagram was plotted using MS Excel spreadsheet, to evaluate variations in hydrochemical facies. Further, multivariate statistical analysis was performed in order to understand the association between variables in the geochemical dataset. Gibb's diagram is used to ascertain the factors controlling the groundwater chemistry of the area. Finally, water quality index for drinking purpose is evaluated and classifications (Table 1) are made as per the WHO and BIS drinking water standards (WHO, 2011; BIS, 2012).

Based on the results of physicochemical analyses, irrigation water quality indices like sodium adsorption ratio (SAR), percent sodium (%Na), magnesium adsorption ratio (MAR), residual sodium carbonate (RSC), Kelly's ratio (KR) and permeability Index (PI) were also calculated.

Multivariate Statistical Analysis

XLSTAT 2018 (version 2018.3.50851) was used for two different statistical analyses, the principal component analysis (PCA) and Pearson correlation coefficients. In order to classify the correlation composition of variables in groundwater chemistry in a better way, PCA was used to augment the understanding of groundwater system and its chemistry. The advantage of statistical analysis is that it converts original variables into uncorrelated variables (PCs) without loss of information. The aim of this analysis is to understand the hydro-geochemistry in observed relations amongst the variables, i.e. the factors. Factors whose eigen value greater than 1 or equal are accepted to detect the possible source of variance in data.

Using Varimax rotation with Kaiser normalization, the components of the PCA were obtained from the dataset by magnifying the summation of the variance of the factor coefficients. This procedure groups variables into different sectors. According to eigen value criterion, only PCs with eigen value greater than or equal to one are considered for interpretation (Kumar et al., 2018). Three principal components having eigen values greater than 1 accounted for 92% of all the data variation which are considered essential and important in the study area.

Pearson correlation coefficients were also computed to examine the interrelation amongst divergent elements so as to classify analogous

Table 1. Statistics of chemical parameters (all in mg/L and EC in $\mu\text{S/cm}$) in groundwater

Variable	Minimum	Maximum	Mean
pH	6.7	8.2	7.27
EC ($\mu\text{S/cm}$)	30	15000	507.585
TDS (mg/L)	19	9000	294.462
TH (mg/L)	16	5600	169.415
NO_3 (mg/L)	0	17	2.391
Turbidity (mg/L)	0	1	0.205
Ca (mg/L)	3	962	30.938
Mg (mg/L)	1	771	22.400
TA (mg/L)	16	1600	75.554
HCO_3 (mg/L)	16	1600	77.385
Cl (mg/L)	8	6400	203.369
Na (mg/L)	5	12595	262.092
K (mg/L)	0	25	0.637
SO_4 (mg/L)	2	800	28.908
%Na (meq/L)	15.21	83.14	40.87
RSC (meq/L)	-105.55	0.059	-2.08
PI (meq/L)	58.16	148.40	102.13
SAR (meq/L)	0.40	73.64	2.46
MAR (meq/L)	21.52	73.28	51.47
KR (meq/L)	0.17	4.93	0.80

sources of elements. Further r value >0.6 is considered as a strong correlation while below that is considered as poor.

RESULTS AND DISCUSSION

Overall Groundwater Chemistry and Quality

Details of the descriptive statistics of the analyzed water quality parameters are shown in Table 1. The pH of water is key to its quality and provides information regarding types of geochemical equilibrium (Hem, 1991). In the study area, the pH varies from 6.7 to 8.2 with a mean of 7.27 (Table 1), indicating a prevailing condition of an alkaline environment (Fig. 3a). However, a few samples, namely 1, 3-5, 21-23, 25-27, 50, 57 and 65, shows the acidic nature with a pH value less than 7. Though pH has no direct effect on human health, all biochemical reactions are sensitive to the variation of this parameter (Subba Rao and Krishna Rao, 1991). The electrical conductivity (EC) indicates the measure of a material's ability to conduct an electric current, the

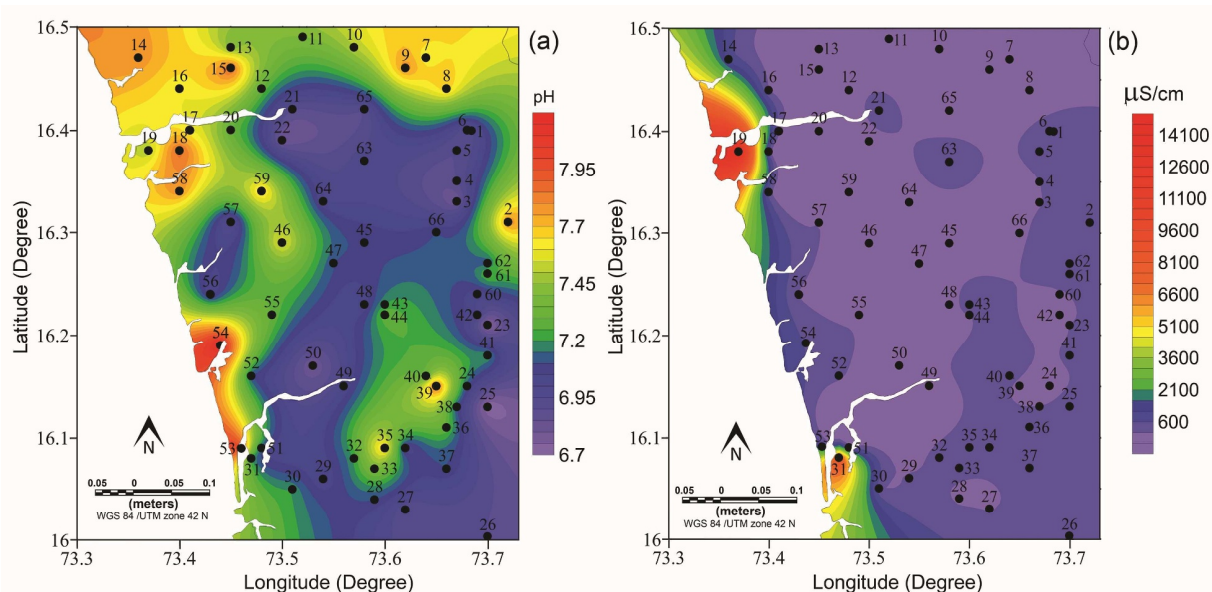


Fig.3. Spatial distribution maps of (a) pH concentration (b) Electrical conductivity concentration.

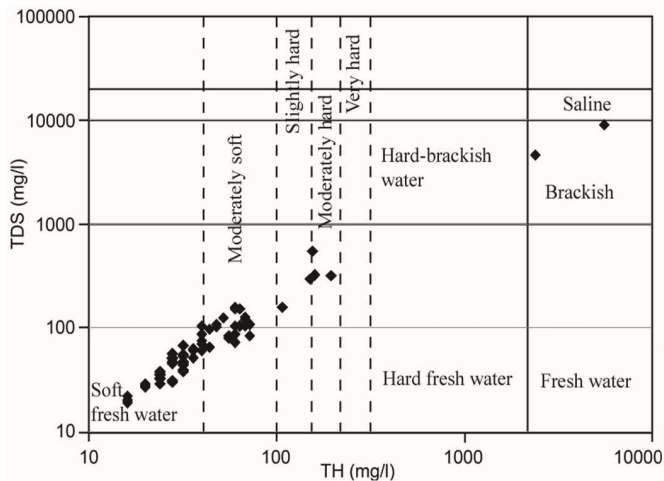


Fig.4. The bivariate plot of TDS versus TH (Total Hardness)

difference of it specifies a wide variation of salts present in the groundwater. In the present study, the EC ranges between 30 and 15000 $\mu\text{S}/\text{cm}$ (Fig.3b) with an average of 507.58 $\mu\text{S}/\text{cm}$, except at two sampling stations (well nos. 19 and 31 in the vicinity of Arabian Sea) where the EC values are in excess of 8,000 $\mu\text{S}/\text{cm}$ (Table 1). Total dissolved solids (TDS) express the degree of salt content, which varies

from 19 to 9000 mg/L with a mean of 294.46 mg/L in the study area. According to Freeze and Cherry (1979), the TDS in groundwater falls under brackish (3.33%) and freshwater (96.67%) in the present study area. Additionally, the bivariate plot of TDS versus TH (Fig. 4) reveals that the majority of the samples (91%) represents “soft freshwater to moderately soft water”, 6% of the sample are of “slightly hard to moderately hard” and the rest 3% signifies the “brackish”, which could plausibly be due to mixing of brackish water with groundwater as because of the location of these samples in proximity to the Arabian Sea.

Major Cations

The excess amount of calcium and magnesium leads to hardness in the water. The concentration of calcium in the water samples varies from 3 to 962 mg/L with an average of 30.9 mg/L (Table 1). According to WHO (2011) and BIS (2012), the acceptable limit of Ca^{2+} content in drinking water is set as 75 mg/L. In the present case, 3% of the samples are above the standard set by WHO and BIS. The concentration of magnesium in the water samples ranges from 1 to 771 mg/L with an average of 22.4 mg/L. The permissible limit of Mg^{2+} content in drinking water is prescribed as 100 mg/L by BIS (2012) and accordingly 3% of samples fall beyond this limit (Figs. 5a,b). All types of groundwater contain relatively small amounts of calcium and magnesium. In general, the maximum amount of Ca^{2+} and Mg^{2+} is derived from calcium rich rocks like carbonates, and gypsum besides from igneous and

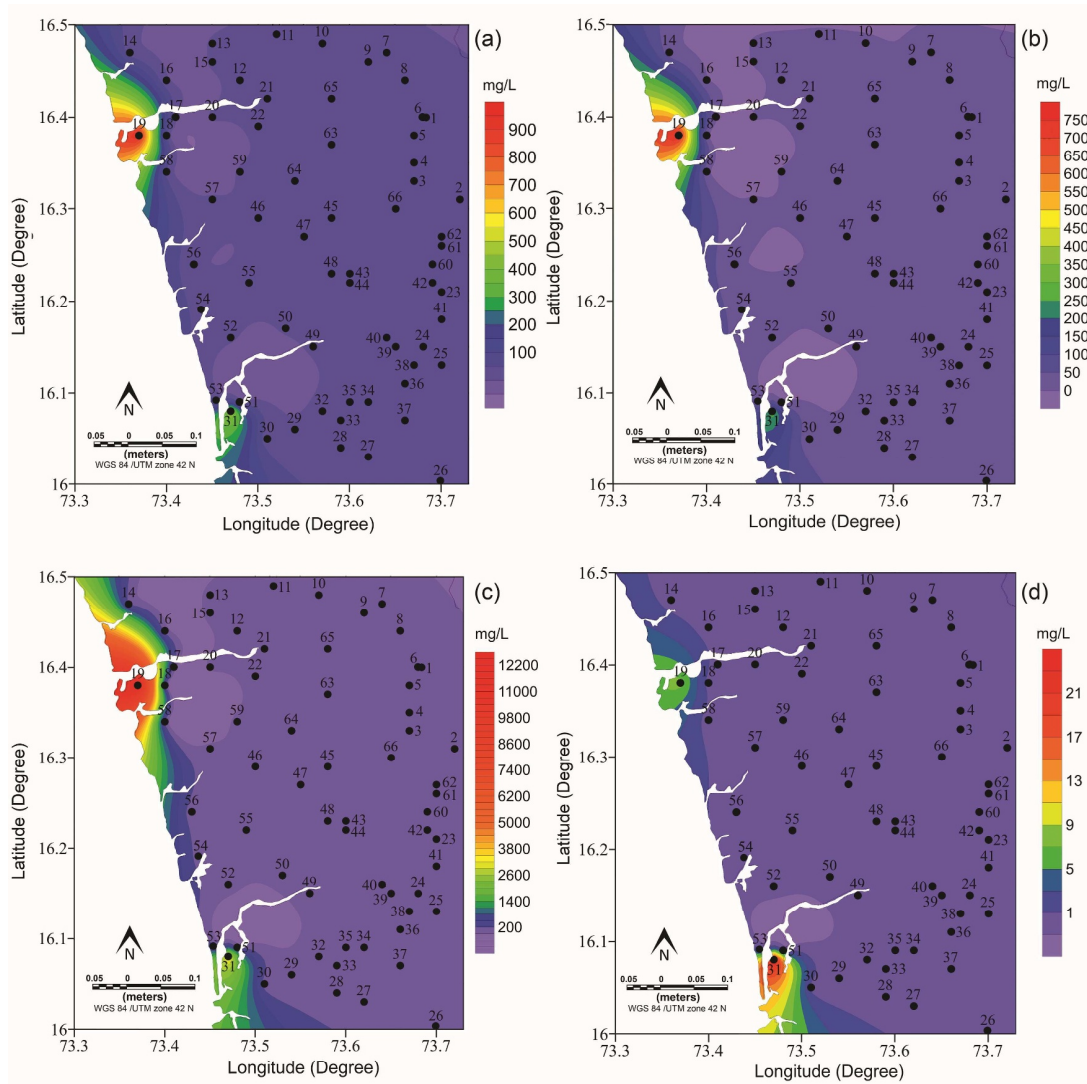


Fig.5. Spatial distribution maps of (a) Ca^{2+} concentration (b) Mg^{2+} concentration (c) Na^{+} concentration (d) K^{+} concentration.

metamorphic rocks due presence of calcium bearing minerals (i.e. anorthite, wollastonite, tremolite and hornblende etc.). It has been reported by Kovalevsky et al. (2004) that magnesite, dolomite, and high-Mg²⁺ calcite in sedimentary deposits are the primary sources of magnesium. However, in cases where groundwater is in interaction with dolomitic or Mg²⁺-rich evaporitic rocks, magnesium is the predominant cation found in groundwater. In this study, the concentration of Ca²⁺ and Mg²⁺ are minimum in most parts of the area (Figs. 5a,b). However, the western part of the study area reveals maximum concentrations of both these cations. As mentioned earlier, sampling sites 19 and 31 are in the vicinity of Arabian Sea and thus the evaporitic rocks formed due to evaporation of seawater producing minerals like gypsum and anhydrite (common salt), enhances the concentration of both Ca²⁺ and Mg²⁺ in this region. Groundwater naturally contains high soluble sodium ion. Though it does not have any significant smell, it imparts an awkward taste to the water at concentrations of 200 mg/L or more (WHO, 2011). The higher amount of Na⁺ in water is likely due to soil leachate, deep saline water, evaporates, cation exchange, seawater intrusion, and industrial waste. The concentration of sodium in the water samples collected varies from 5 to 12595 mg/L, with an average of 262.09 mg/L. It is observed that except at sampling points 19 and 31, all others are within the permissible limit (WHO, 2011) (Fig. 5c). In contrast to the concentrations amongst the cations, the K⁺ content is observed to be

low, (varying between 0.1 and 25.3 mg/L, with a mean of 0.637 mg/L) (Fig. 5d). The fairly low concentrations of ionic potassium in groundwater are because of more resistance to decomposition by weathering processes (Hem, 1991).

Major Anions

Chloride in groundwater is contributed by both natural and anthropogenic sources, as it is derived mainly from non-lithological sources (viz. poor sanitary conditions, irrigation return-flows, chemical fertilizers etc.), and seawater intrusion in coastal areas (WHO, 2011). In the study area, the concentration of Cl⁻ varies from 8 to 6400 mg/L, with an average of 203.37 mg/L (Table 1). The permissible limit of chloride in drinking water has been set as 200 mg/L (WHO, 2011). In the present situation, all samples are within the permissible limit except 3 samples (well nos. 15, 19 and 31). The high values along the coastal tracts at well 19 and 31 are due to seawater intrusion. The high value at sampling well 15 is presumably due to the seepage of rural sewage into the groundwater (Fig. 6a). The concentration of bicarbonate in the water samples varies from 16 to 1600 mg/L, with an average of 72.38 mg/L (Table 1). The higher values of HCO₃⁻ are seen at sampling points 19 and 31 (Fig. 6b), indicating the dominance of mineral dissolution due to decaying of organic matter (Stumm and Morgan, 1996). It is observed that CO₃²⁻ is below the detectable limit in all the water samples. The concentration of SO₄²⁻ is observed to be ranging

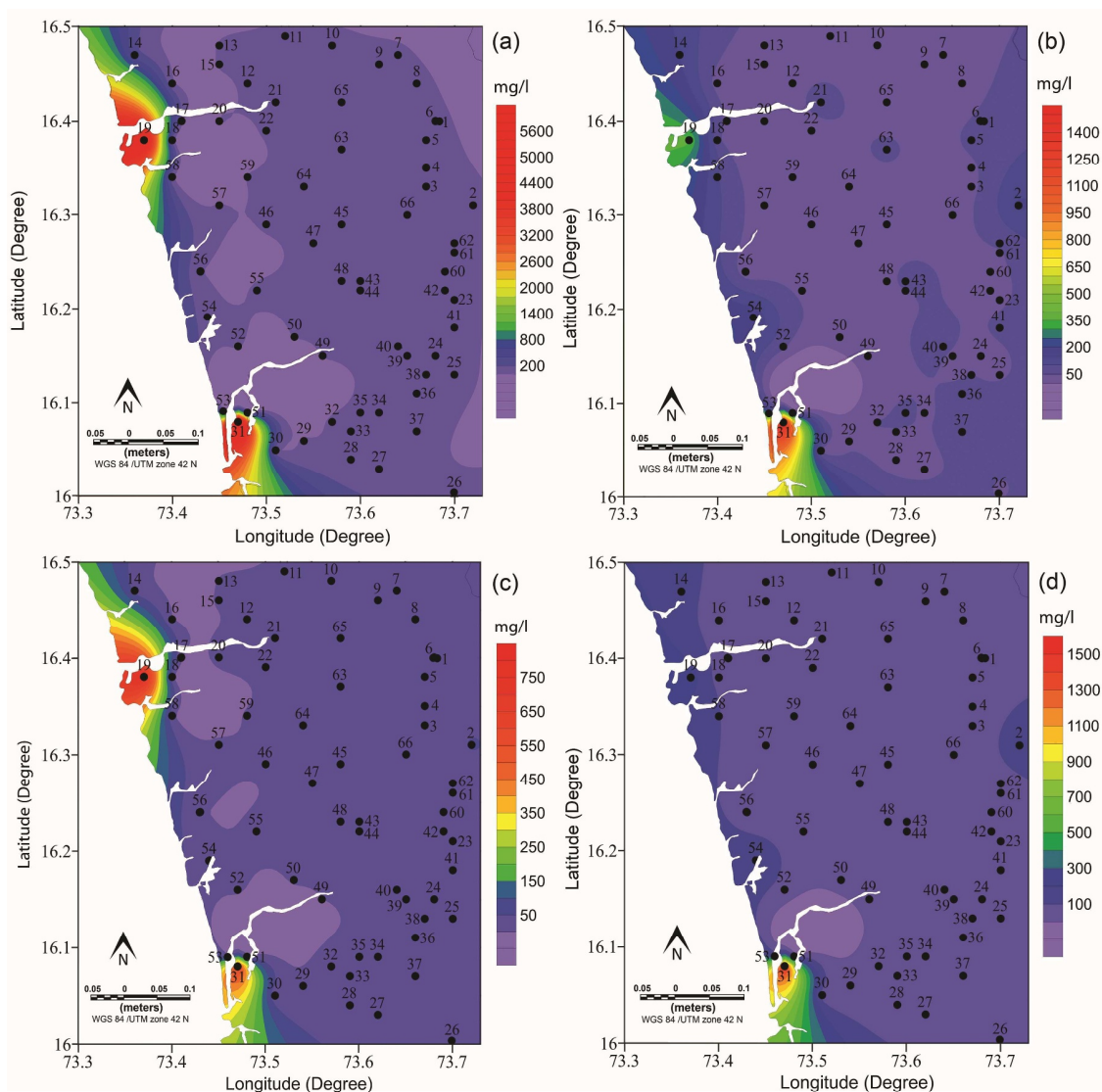


Fig.6. Spatial distribution maps of (a) Cl⁻ concentration (b) HCO₃⁻ concentration (c) SO₄²⁻ concentration (d) Total alkalinity concentration.

from 0 to 800 mg/L (Table 1), with a mean of 28.90 mg/L. Sulphate ions do not have any significant detrimental role on humans and animals. It is an essential nutrient for plants. At levels above 1000 mg/L, sulphate in drinking water can have a laxative effect. The standard limit of sulphate in drinking water is 200 mg/L (WHO, 2011), and all the studied samples have values less than 200 mg/L, except 2 samples [well nos. 19 (800 mg/L) and 31 (637 mg/L)] (Fig. 6c).

In order to identify the amount of natural salts present in the water, the total alkalinity (TA) is measured. The alkalinity of water is its capacity to neutralize a strong acid and it is normally due to the presence of bicarbonates, carbonates and hydroxide compounds of calcium, sodium and potassium. According to BIS (2012), the permissible limit of TA in groundwater ranges between 200 and 600 mg/L. The total alkalinity values of all the investigated samples were found to be within the limit, except for the samples 19 and 31 (Table 1, Fig. 6d). A large amount of alkalinity in water imparts a bitter taste and is harmful for irrigation as it damages soil texture and hence reduces crop yield (Sundar and Saseetharan, 2008).

Evaluation of Hydrogeochemical Facies and Dominant Controlling Processes

The major cations and anions of the groundwater samples depend largely on the geology as well as on the geochemical processes which take place within the groundwater system. Spatial mapping of groundwater facies can help in understanding the hydrogeochemical properties and analyze the water composition. In the present study, the groundwater samples were classified hydrochemically using major cations and anions with conventional Piper trilinear diagram (1944) and Chadha's plot (1999) to determine the variation in hydrochemical facies. As is evident from the Piper plot (Fig. 7) that the dissemination of cations in the mixed zone, except a few samples, which shows moderate to strong $\text{Na}^+\text{+K}^+$ dominance. Whereas, the anions predominantly fall between the bicarbonate and mixed zone dominance excluding three samples (14, 19 and 31), which are showing strong Cl^- dominance (Fig. 6a). Not much variation is observed in the distribution of cations and anions in the study area, suggesting its similar chemical characteristics. The diamond shape field reveals that barring three samples (14, 19 and 31), most of the water samples are characterized by $\text{Ca}^{2+}\text{-HCO}_3^-$, typical of shallow and fresh groundwater facies and mixed $\text{Ca}^{2+}\text{-Mg}^{2+}\text{-Cl}^-$ type. While the rest of three samples show $\text{Na}^+\text{-Cl}^-$ facies, indicating high salinity and typical of marine and deep ancient groundwater. In order to classify the hydrogeochemical evolution and their possible pathways in the study area Chadha's diagram (Chadha, 1999) was also used. This is obtained in terms of the percentages of major cation and anion and water types which are represented in each of the four quadrants of the graph. Figure 8 represents the graphical illustration of four quadrants of concentration and is expressed as the difference between alkaline earths ($\text{Ca}^{2+}\text{+Mg}^{2+}$) and alkali elements ($\text{Na}^+\text{+K}^+$) for cations and the difference between weak acids (HCO_3^-) and strong acids ($\text{Cl}^- \text{+SO}_4^{2-}$). The four quadrants of the graph are broadly designated as the recharging water ($\text{Ca}^{2+}\text{-Mg}^{2+}\text{-HCO}_3^-$ type) in the first quadrant, reverse ion exchange water ($\text{Ca}^{2+}\text{-Mg}^{2+}\text{-Cl}^-$ type) in the second quadrant, seawater ($\text{Na}^+\text{-Cl}^-$ type) in the third quadrant and base ion exchange water ($\text{Na}^+\text{-HCO}_3^-$ type) in the fourth quadrant. It can be observed from Fig. (8) that 38 samples fall in quadrant 1 which is recharging water type. This is due to the fact that the water samples were collected during post monsoon period and thus when water infiltrates into the ground from the surface, it carries dissolved carbonate (HCO_3^-) and the potable Ca^{2+} , and therefore a large number of samples fall in quadrant 1. Eighteen samples fall in quadrant 2, indicating reverse ion exchange water of $\text{Ca}^{2+}\text{-Mg}^{2+}\text{-Cl}^-$ type. It may be inferred that $\text{Ca}^{2+}\text{+Mg}^{2+}$ is in excess to $\text{Na}^+\text{+K}^+$ due to discharge of Ca^{2+} and Mg^{2+} from weathering of minerals. Even though ten samples fall in the third quadrant, i.e. seawater type, about 7 of

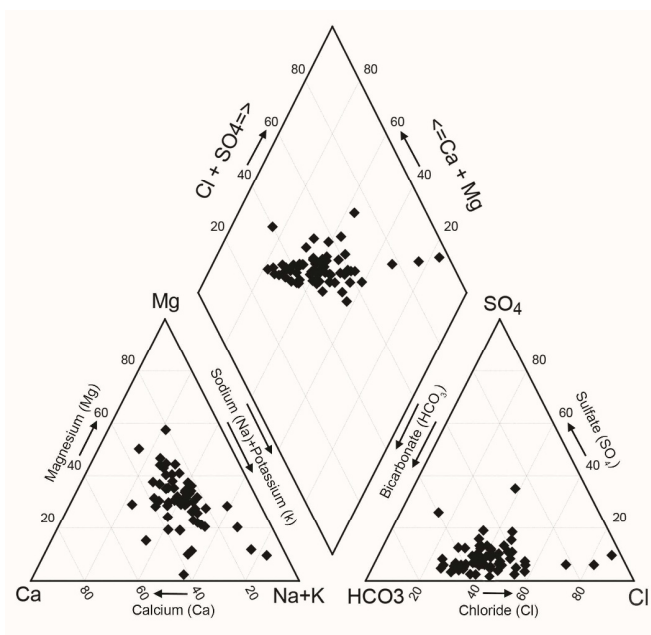


Fig.7. Piper trilinear diagram showing chemical characteristics of groundwater and hydrochemical facies.

them exhibit strong acidic anions which exceed weak acidic anions. The remaining 3 samples strongly exhibit the sodium chloride type ($\text{Na}^+\text{-Cl}^-$) water which could be due to typical seawater mixing resulting due to the proximity of Arabian Sea. Quadrant 4 ($\text{Na}^+\text{-HCO}_3^-$) type waters are not prominent in the study area.

In order to detect the mechanism which controls the groundwater chemistry of the study area, Gibbs diagram was used (Gibbs, 1970). This is extensively used to get the probable sources of dissolved chemical constituents in aquifer, essentially from three different fields such as, atmospheric precipitation, evaporation and rock-water interaction (Gibbs, 1970). The chemical analysis of the samples is shown in Figs. (9a, b). The results suggest that all the water samples fall predominantly in the rock dominance field with inclination towards precipitation dominance and this might be due to chemical weathering of rocks with infiltrating precipitated water while circulating into the subsurface (Singh et al., 2017). Whereas, three samples (14, 19 and 31) fall in evaporation dominance field, which are attributed to the effect of seawater intrusion that enhances the salinity by increasing the concentration of Na^+ and Cl^- .

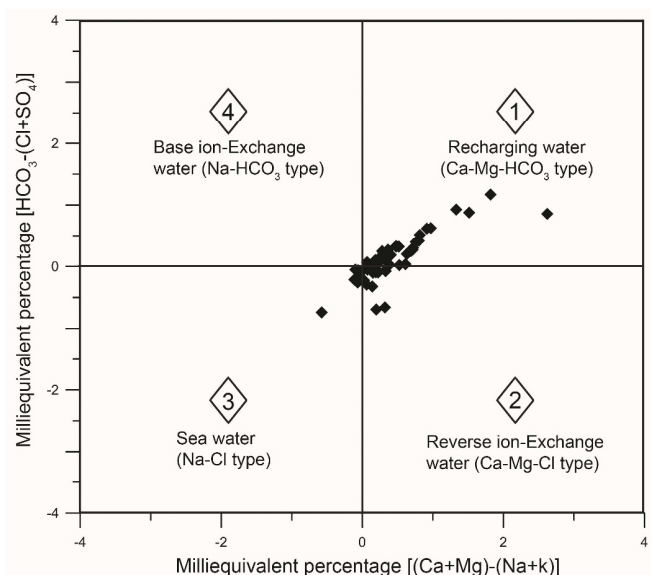


Fig.8. Chadha's diagram of geochemical samples classification.

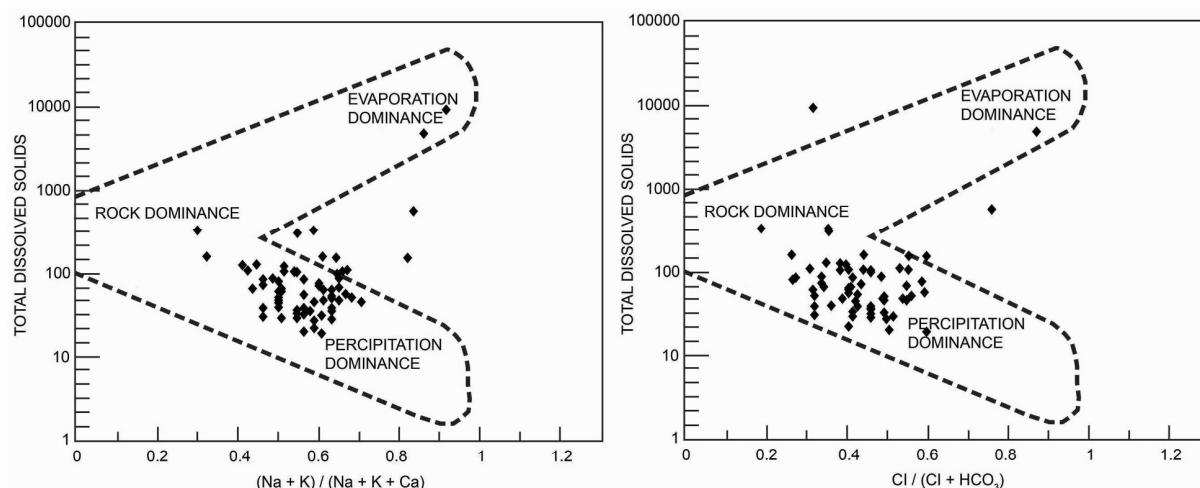


Fig.9. Gibb's diagram of geochemical samples plotted in semi-log graph.

Sodium versus chloride molar ratio is one of the good indicative factors of evaporation and ion exchange in groundwater. It is apparent from the plot $(\text{Na}^+/\text{Cl}^-)$ versus EC (Fig. 10a) that most of the samples having $\text{Na}^+/\text{Cl}^- > 1$ shows inclined trend with $\text{EC} < 1000 \mu\text{S}/\text{cm}$ and are indicative of dissolution or ion exchange reaction dominating over evaporation. In contrast, three samples plotted parallel to the EC axis with high EC values ($> 10000 \mu\text{S}/\text{cm}$) indicate the effect of sea water intrusion into the groundwater. The bivariate plot made between $\text{Mg}^{2+}/\text{Na}^+$ vs $\text{Ca}^{2+}/\text{Na}^+$ on log-log scale (Fig. 10b) indicates that majority of the samples fall in the silicate weathering field as because of lower molar ratios (both $\text{Mg}^{2+}/\text{Na}^+$ and $\text{Ca}^{2+}/\text{Na}^+$ ratios < 1). These lower molar ratios are ascribed to the rock-water interaction of silicates / schistose rocks (quartz, chlorite, amphibolites, schist etc.) in groundwater. On the other hand, slightly higher values of the ratios indicate the effect of salinity with abnormal behavior rather than carbonate dissolution. Most of the samples in this study fall around the 1:1 equi-line $(\text{Ca}^{2+} + \text{Mg}^{2+})$ vs $(\text{SO}_4^{2-} + \text{HCO}_3^-)$ (Fig. 10c), suggesting that carbonate and silicate weathering are the major hydrogeochemical process operating in this region. Likewise, the $\text{Ca}^{2+}/\text{Mg}^{2+}$ molar ratios for 60.61% samples are less than 1 deduce the effect of dolomite mineral dissolution by the rock-water interaction (Fig. 10d), 31.82% samples lies within 1-2 ratio explains the role of Ca and Mg bearing minerals from mafic rock units, calcite, gypsum mineral dissolution that leads to excess Ca into the groundwater system at these places of the study area. Whereas, only a few samples (around 7.58%) are indicative of the silicate mineral dissolution. In order to recognize the effect of salinization in groundwater, the molar ratio of $\text{Cl}^-/\text{HCO}_3^-$ (being the best indicator of salinization due to the seawater encroachment) has been used to characterize the type of water and thus the origin of salinity in groundwater (Todd, 1959). The molar ratio of $\text{Cl}^-/\text{HCO}_3^- < 0.5$ suggest unaffected groundwater, 0.5-6.6 shows slightly or moderately affected, and > 6.6 specifies strongly affected salinization in groundwater. The plot (Fig. 10e) between Cl^- and $\text{Cl}^-/\text{HCO}_3^-$ indicates 10% of the samples are unaffected by saline water intrusion and 86% of the groundwater samples are slightly to moderately affected (0.5 to 1.5) by the mineral dissolution and weathering of rocks. The remaining samples are strongly affected by seawater intrusion, as these wells are located near the backwaters and fall in the vicinity of Arabian Sea.

Furthermore, $\text{NO}_3^-/\text{Cl}^-$ versus Cl^- provide the impact of anthropogenic pollution apart from that of seawater encroachment and mixing with groundwater. Barring three samples, all the samples with lower $\text{NO}_3^-/\text{Cl}^-$ molar ratios and NO_3^- concentration (Fig. 10f) fall under the permissible limit of 45 mg/L set by BIS (2012). The three samples with elevated chloride concentration and lower $\text{NO}_3^-/\text{Cl}^-$ molar

ratios indicate the salinization of groundwater by seawater encroachment.

Chemometric Methods

Principal Component Analysis

The results of varimax orthogonal rotated component matrix including factor loadings, eigenvalues, percentage of variance and cumulative percent for first three components considered in this study are summarized in Table 2, wherein, the first principal component (PC1) accounts for 71.31% of total variance and depicts very strong positive loadings in EC, TDS, Cl^- , Na^+ , K^+ , SO_4^{2-} , TH, Turbidity, Ca^{2+} , Mg^{2+} , Total alkalinity and HCO_3^- , primarily due to weathering effect. Being a coastal area, salinity factor is reflected in PC1 as high positive loading in Na^+ and Cl^- , which is derived from rock water interaction due to weathering of minerals in groundwater. It is observed that in PC1 the strong positive correlation between Ca^{2+} and Mg^{2+} (Table 2) is due to dominance of mafic rock weathering, besides dolomite, calcite, gypsum mineral dissolution in the study area.

The second component (PC2) is observed to account for 12.38% (eigenvalue) and 12.38% of total variance. The positive loading of HCO_3^- , Total alkalinity and K^+ in the PC2 explains their natural occurrence in the water plausibly due to weathering of potassium feldspar mineral bearing schistose rocks (quartz, chlorite, amphibolites,

Table 2. Varimax orthogonal rotated loadings from Principal component analysis (PCA) of standardized water quality parameters

	PC1	PC2	PC3
pH	0.064	-0.130	0.775
EC	0.987	-0.157	-0.009
TDS	0.970	-0.238	-0.017
TH	0.950	-0.310	-0.030
NO_3^-	-0.001	-0.176	0.708
Turbidity	0.853	0.163	-0.149
Ca	0.966	-0.254	-0.023
Mg	0.934	-0.353	-0.035
Total alkalinity	0.737	0.659	0.130
HCO_3^-	0.783	0.604	0.123
Cl	0.984	0.160	0.012
Na	0.899	-0.433	-0.058
K	0.839	0.528	0.055
SO_4	0.997	-0.044	-0.011
Eigenvalue	9.984	1.734	1.165
Variability (%)	71.314	12.383	8.323
Cumulative %	71.314	83.697	92.020

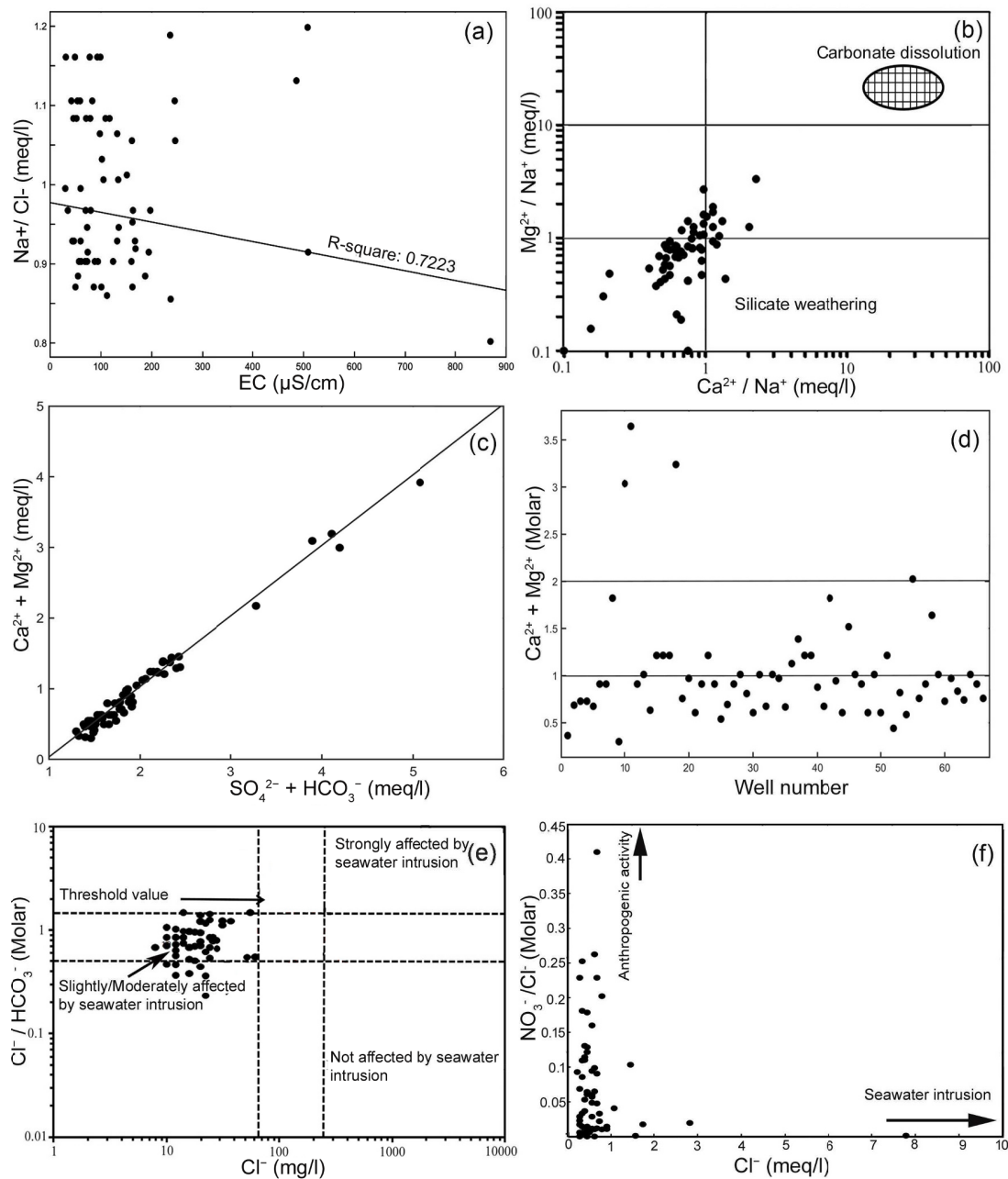


Fig.10. (a) The ratio plots of a Na^+/Cl^- (meq/L) vs EC ($\mu\text{S}/\text{cm}$). (b) The bivariate plot of $\text{Mg}^{2+}/\text{Na}^+$ (meq/L) vs $\text{Ca}^{2+}/\text{Na}^+$ (meq/L). (c) The bivariate plot of $\text{Ca}^{2+}+\text{Mg}^{2+}$ (meq/L) vs $\text{SO}_4^{2-}+\text{HCO}_3^-$ (meq/L). (d) Molar ratio plot of $\text{C}_g^{2+}/\text{Mg}^{2+}$ vs sample in the study area. (e) The relationship between $\text{Cl}^-/\text{HCO}_3^-$ vs Cl^- concentration in the study area. (f) $\text{NO}_3^-/\text{Cl}^-$ versus Cl^- indicating seawater intrusion.

schist, etc.) and gneisses, which are adjacent and in up-dip direction of the wells situated in the vicinity of the coast. The final component (PC3) with eigenvalue 1.16 and 8.32% variance exhibits strong positive loadings by pH and NO_3^- and this can be attributed to anthropogenic contamination such as the utilization of nitrate rich fertilizers for irrigation purpose and domestic waste disposal contributed to NO_3^- content into the groundwater system. However, the nitrate concentration reported in the study area is within the permissible limit of BIS (2012) guidelines (i.e. <45 mg/L) and therefore no harm to the populace in view of potable use.

Correlation Analysis

Pearson correlation coefficients between the physico-chemical parameters for water quality studies are shown in Table 3. It is seen from the table that EC has strong correlation with TDS ($r = 0.99$), TH

($r = 0.98$), Mg^{2+} (0.99), Ca^{2+} (0.97), Cl^- (0.94), Na^+ (0.95) and SO_4^{2-} (0.99). Likewise TDS also shows strong correlation among these elements. These strong associations of EC and TDS with other parameters reveal their contribution in mineralization of water. Generally EC and TDS increases with increase in dissolved solids in water, thereby exhibiting a strong correlation of interdependency.

It can be observed from Table 3 that TH also exhibits a strong correlation with Ca^{2+} (0.99), Mg^{2+} (0.99), Turbidity (0.74), Cl^- (0.88), Na^+ (0.99) and SO_4^{2-} (0.96). Robust correlation between these parameters is due to calcite and dolomite dissolution, weathering process, rock water interaction and mineral precipitation. TH with respect to Ca^{2+} and Mg^{2+} suggests that the two cations probably contribute most to hardness of water in the study area. Calcium shows good correlation with Mg^{2+} (0.99), Na^+ (0.98), Cl^- (0.91) and SO_4^{2-} (0.97), while Mg^{2+} also suggests strong positive correlation with these

Table 3. Pearson's correlation matrix for study area groundwater samples

Variables	pH	EC	TDS	TH	NO ₃	Turbidity	Ca	Mg	TA	HCO ₃	Cl	Na	K	SO ₄
pH	1	0.077	0.085	0.082	0.156	-0.097	0.081	0.084	0.062	0.068	0.039	0.072	0.003	0.056
EC	0.077	1	0.996	0.987	0.014	0.800	0.994	0.978	0.625	0.679	0.947	0.956	0.746	0.992
TDS	0.085	0.996	1	0.997	0.020	0.776	0.999	0.992	0.559	0.617	0.917	0.977	0.687	0.979
TH	0.082	0.987	0.997	1	0.024	0.749	0.998	0.999	0.494	0.555	0.884	0.990	0.632	0.961
NO ₃	0.156	0.014	0.020	0.024	1	-0.063	0.020	0.027	-0.031	-0.028	-0.012	0.027	-0.034	0.000
Turbidity	-0.09	0.800	0.776	0.749	-0.063	1	0.771	0.731	0.691	0.722	0.839	0.693	0.764	0.824
Ca	0.081	0.994	0.999	0.998	0.020	0.771	1	0.994	0.544	0.602	0.911	0.981	0.677	0.976
Mg	0.084	0.978	0.992	0.999	0.027	0.731	0.994	1	0.454	0.517	0.862	0.995	0.594	0.948
TA	0.062	0.625	0.559	0.494	-0.031	0.691	0.544	0.454	1	0.997	0.831	0.371	0.971	0.705
HCO ₃	0.068	0.679	0.617	0.555	-0.028	0.722	0.602	0.517	0.997	1	0.868	0.437	0.981	0.754
Cl	0.039	0.947	0.917	0.884	-0.012	0.839	0.911	0.862	0.831	0.868	1	0.816	0.920	0.976
Na	0.072	0.956	0.977	0.990	0.027	0.693	0.981	0.995	0.371	0.437	0.816	1	0.525	0.917
K	0.003	0.746	0.687	0.632	-0.034	0.764	0.677	0.594	0.971	0.981	0.920	0.525	1	0.817
SO ₄	0.056	0.992	0.979	0.961	0.000	0.824	0.976	0.948	0.705	0.754	0.976	0.917	0.817	1

parameters (Table 3). The strong correlation between Ca²⁺ and Mg²⁺ with other parameters can be attributed not only to the carbonate rocks present in the area, but also probably from Mg-bearing mineral in the basaltic terrain. Total alkalinity shows strong correlation with HCO₃⁻ (0.99), Cl^e (0.83), SO₄²⁻ (0.70) and K⁺ (0.97). Silicate and carbonate weathering are the primary sources for the enhancement of SO₄²⁻ and K⁺. Sodium indicates good positive correlation with the Cl⁻ (0.81) and SO₄²⁻ (0.91). It is reported that dissolution of halite is an important process of mineralization (Hem, 1991), which might be the cause for high correlation between Na⁺ and Cl⁻. Being a coastal region, saline water intrusion may also be a causative factor for the strong correspondence observed between Na⁺ and Cl⁻.

Groundwater Quality Index for Drinking Purpose

To assess the groundwater quality for drinking purpose, Water quality index (WQI) was computed, which gives a measure of holistic qualitative nature of water. The computation for water quality for drinking purpose was carried out with reference to the standards given by World Health Organization (WHO, 2011; BIS, 2012). For calculation of WQI, 11 vital physico-chemical parameters (namely pH, electrical conductivity, total dissolved solids, total hardness, alkalinity, calcium, magnesium, sodium, potassium, chloride and sulphate) have been considered (Table 4). Hence for the present calculation, each of the chemical parameter was assigned weights (w_i) depending on the overall assignment for drinking water quality. The maximum weight of 5 is assigned to those parameters which have major impact on the water quality, on the other hand, minimum weight 1 is assigned to those parameters which are not harmful for consumption (Singh et al., 2017b). The following equations are employed for calculating WQI.

The unit weight (W_i) of nth parameters is calculated by Eq. (1),

$$W_i = \frac{w_i}{\sum_{i=1}^n w_i} \tag{1}$$

Table 4. Water quality classification based on WQI value (after Chatterjee and Razuddin, 2002)

Range of values	Category	Groundwater locations
<25	Excellent water	1, 3-13, 15-18, 20-30, 32-52, 55-60
26-50	Good water	2, 53, 54
51-75	Poor water	14
76-100	Very poor water	—
>100	Unsuitable	19, 31

The quality rating (Q_i) for each parameter was calculated by Eq. (2)

$$Q_i = (V_{sample} - V_{ideal}) / (V_{standard} - V_{ideal}) * 100 \tag{2}$$

In Eq. (2) V_{sample} is the estimated value of the sample at a particular sampling station; V_{standard} is the standard permissible value of each parameter (WHO, 2011; BIS, 2012) and V_{ideal} is the ideal value of each parameter (i.e. 0 for all other parameters except pH which has value of 7).

The Water Quality Index (WQI) was calculated by using Eq. (1) and (2) as,

$$WQI = \sum (Q_i * W_i) \tag{3}$$

In this study, thematic representation of water quality data over space for water quality zonation is performed on the basis of WQI. The study area has been categorized into five different parts depending on WQI, like “excellent” (WQI <25), “good” (WQI 26–50), “poor” (WQI 51–75), “very poor” (WQI 76–100), and “unsuitable” (WQI >100) (Chatterjee and Razuddin, 2002). Table 5 shows how many of the total water samples that falls under each of the category.

The values of GWQI in the study area range between 3.59 and 1615.28. Though most of the groundwater samples (96%) fall under the ‘excellent’ to ‘good’ category, nearly 4% of the samples [well numbers 14 (61.9), 19 (1615) and 31 (894.9)] are categorized as ‘poor to unsuitable’ (Fig. 11).

Irrigation Water Quality

Evaluation of water quality for irrigation is essential for the yield and health of crops, maintenance of soil productivity and protection of the environment (Li et al., 2013; Singh et al., 2013). Excess concentration of dissolved ions in water can affect plants as well as the physico-chemical properties of soils, which would lead to lower productivity and destruction of soil structure (Ravikumar et al., 2010). Assessment of irrigation water quality is a measure of the salt concentration which is estimated by EC and relative amount of Na⁺. This include sodium adsorption ratio (SAR), sodium percentage (%Na), residual sodium carbonate (RSC), magnesium adsorption ratio (MAR), and Kelly’s ratio (KR) and permeability index (PI) (Ramesh and Elango, 2011; Singh et al., 2012). Percent sodium and EC plays a vital role which can control the use and classification of groundwater for irrigation.

Sodium Adsorption Ratio (SAR)

EC and Na⁺ are the key parameters to signify the quality of water

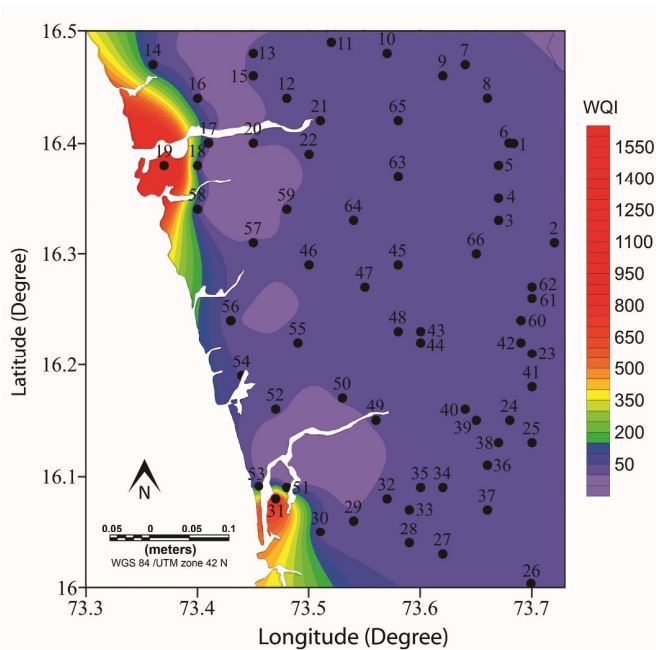


Fig.11. Spatial distribution map of drinking water quality index.

used for irrigation. The sodium adsorption ratio (SAR) can be used as an index for determining the alkaline nature of soil and the risks associated with it. SAR is calculated from the formula given by Richards (1954) where all the ion values are in meq/L.

$$SAR = \frac{Na^+}{\sqrt{(Ca^{2+} + Mg^{2+})/2}} \quad (4)$$

The values of SAR for groundwater samples range from 0.407 to 73.6 (Table 1). The water samples having SAR values less than 10 are considered excellent, 10–18 as good, 18–26 as fair (doubtful) and above 26 as unsuitable for irrigation use (USDA, 1954). In present case most of the samples fall in excellent category except two samples, well 19 and 31, where the SAR values are 73.6 and 31.2 respectively, and thus unsuitable for irrigation purpose.

In the present study, the SAR values are plotted against EC values (USSL, 1954) to obtain the water quality based on salinity and sodium hazard classification (Fig. 12). Most of the groundwater samples fall under low salinity to low sodium type water (C1–S1 category), whereas very few groundwater samples are categorized as medium salinity to low sodium type C2–S1. Only one sample fall under high salinity to low sodium type C3–S1. It may be noted that two samples (not shown in Fig. 12) fall in very high salinity to very high sodium type of water.

Percent Sodium (%Na)

Concentration of sodium is particularly critical while evaluating the suitability of water for irrigation purposes. Higher concentrations of sodium in water cause flocculation and clogging of inter-granular matrix in soil, leading to reduction of soil permeability, thereby causing degradation of soil (Hamill and Bell, 1986). %Na is computed with respect to the concentration of other major cations (meq/L) using Eq. (5) given by Wilcox (1955).

$$\%Na = \frac{(Na^+ + K^+) * 100}{(Ca^{2+} + Mg^{2+} + Na^+ + K^+)} \quad (5)$$

In the study area, the %Na lies between 15.2 and 83.14% (Table 1) with an average of 40.87%. As per BIS (2012), the recommended level of %Na is up to 60%, beyond which the water is unfit for irrigation. The Wilcox plot of EC versus %Na (Fig. 13) reveals that

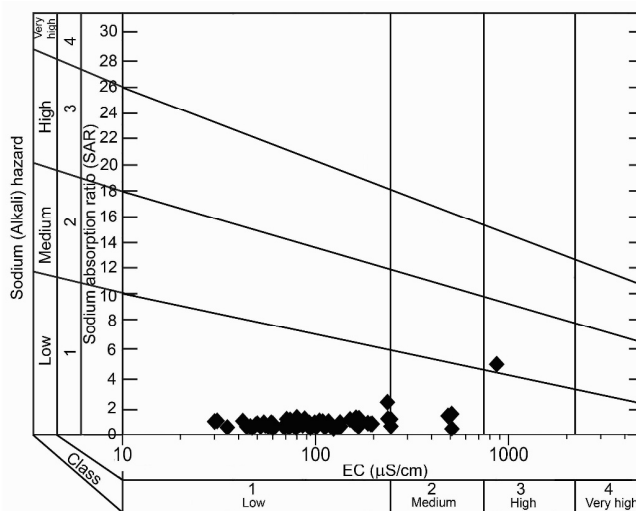


Fig.12. US Salinity diagram indicating the suitability of groundwater for irrigation use.

97% of groundwater samples fall under excellent to good category, with few samples falling under permissible to unsuitable category (well nos. 14, 19 and 31). However, due to very high EC and other associated cation values, the sample numbers 19 and 31 are not marked in Fig. 13.

Magnesium Adsorption Ratio (MAR)

Magnesium adsorption ratio (MAR) is computed using Eq. (6) (Szabolcs and Darab, 1964),

$$MAR = \frac{Mg^{2+}}{(Ca^{2+} + Mg^{2+})} \times 100 \quad (6)$$

where all the ion values are expressed in meq/L. Excess amount of magnesium in irrigation water adversely effects the soil quality (Kumar et al., 2007). MAR values in the study area ranges between 21.52 and 73.28 with an average 51.47 (Table 1). It is reported that if MAR value is more than 50, such waters are considered to be risky for irrigation due to its adverse effect on crop yields (Paliwal, 1972). In the present study 60% of water samples are unsuitable and the remaining 40% are suitable for irrigation.

Residual Sodium Carbonate (RSC)

Excess precipitation or dissolution of alkaline earth carbonates

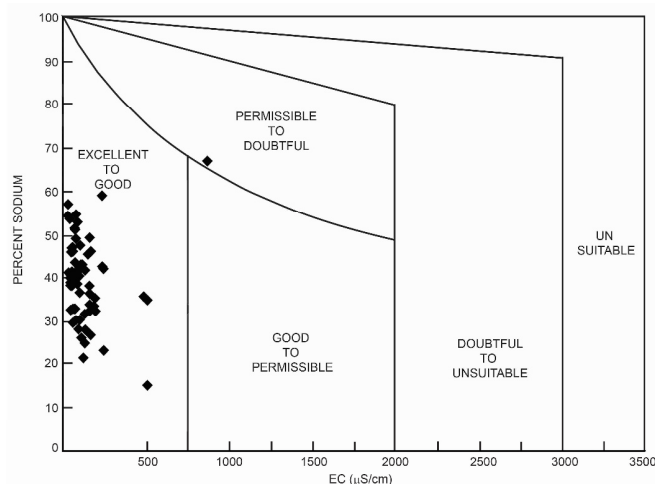


Fig.13. Percent sodium and electrical conductivity plot (after Wilcox, 1955).

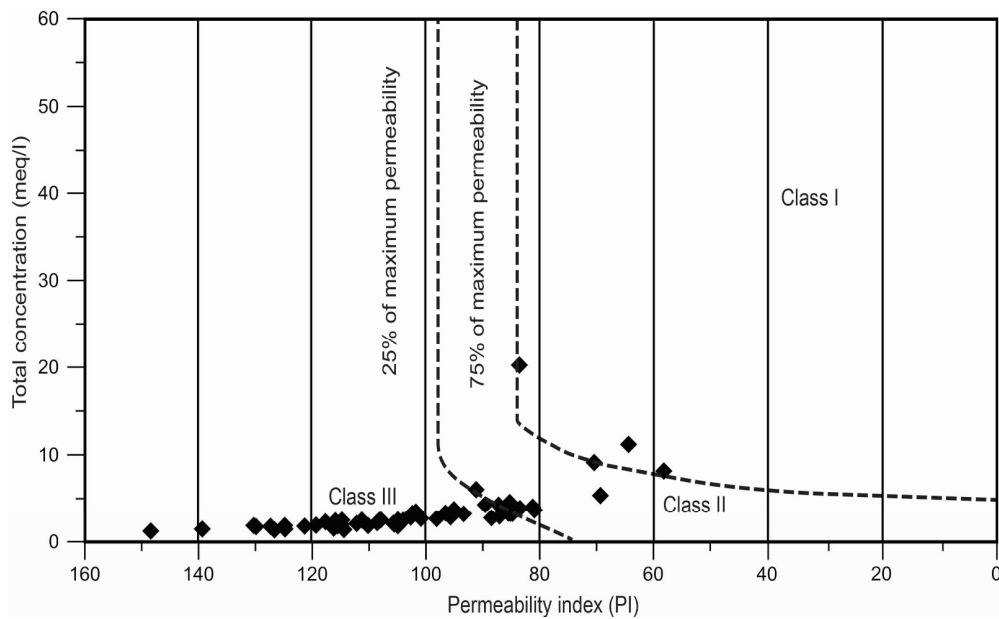


Fig.14. Doneen's chart representing classification of groundwater for irrigation use.

changes the concentration of calcium and magnesium which affects the SAR content in the soil. Carbonate deposition is more intense in groundwater. Groundwater with a partial pressure of CO_2 and a high concentration of bicarbonate is in equilibrium, but once it is extracted and exposed to free air, CO_2 is released and calcium and magnesium are deposited as carbonate (Eaton, 1950). In this process, all calcium and magnesium ions are precipitated as carbonate and the amount of residual sodium carbonate (RSC) can be calculated using Eq. 7. All concentrations are expressed in meq/L (Eaton, 1950).

$$RSC = (CO_3^{2-} + HCO_3^-) - (Ca^{2+} + Mg^{2+}) \quad (7)$$

Generally RSC can be classified as suitable, if it is less than 1.25 meq/L; marginally suitable, if the value is between 1.25 and 2.50 meq/L; and unsuitable, if it is higher than 2.50 meq/L. In present study area all samples except one (sample no. 19) fall under suitable category (Table 1).

Kelly's Ratio

Kelly's ratio (KR) is calculated as the ratio of sodium with respect to calcium and magnesium (Eq. 8) (Kelly, 1957), where all concentrations are in meq/L.

$$KR = \frac{Na^+}{(Ca^{2+} + Mg^{2+})} \quad (8)$$

The KR values exceeding 1 indicate an excess of sodium concentration, while values less than 1 signify waters suitable for irrigation. The groundwater samples in the study area have KR values varying from of 0.177-4.93, with an average 0.8 (Table 1). It can be observed that about 83% of groundwater is suitable for irrigation while remaining 17% is unsuitable due to increase of Na^+ against Ca^{2+} and Mg^{2+} ions, which decreases soil permeability thus affecting crop yield.

Permeability Index

Doneen (1964) calculated the permeability index (PI) based on the Eq. 9. All concentrations are in meq/L.

$$PI = \frac{Na^+ + \sqrt{HCO_3^-}}{(Ca^{2+} + Mg^{2+} + Na^+)} \times 100 \quad (9)$$

PI of soil is affected by calcium, magnesium, sodium and bicarbonate contents of irrigation water. PI varies from 58.16 to 148.4 with an average value of 102.4. Doneen's diagram was prepared for the 66 sample as shown in Fig. (14). It is seen from the figure that 4 samples are in Class I category (>75% permeability), 9 samples are in Class II category (25-75% permeability) and remaining all fall in Class III category (<25% permeability). The above result reveals that around 80% of the water samples fall in the Class III category, indicating the fact that excess use of such water drastically decreases the permeability of soil which make the soil hard and thus unfit for irrigation.

Irrigation Water Quality Index

Water quality for irrigation was calculated using the procedure that was adopted for drinking water quality index discussed earlier. The parameters considered for irrigation water quality index are pH, EC, sulphate, SAR, %Na, RSC, PI, MAR and Kelly's ratio. The

Table 5. Parameters desirable limits assigned weights references

	Desirable limits	Assigned weights	References
pH	8.5	0.0370	BIS (2012)
EC(μ S/cm)	1500	0.074	Freeze and Cherry (1979)
RSC (meq/L)	2.5	0.111	Eaton (1950)
Permeability Index	85	0.111	Domenico and Schwartz (1990)
SAR	18	0.111	Richard (1954)
Sulphate (meq/L)	4.2	0.148	BIS (2012)
%Na	60	0.148	Wilcox (1955)
MAR	50	0.074	Szabolcs and Darab (1964)
Kelly's Ratio	1	0.185	Kelly (1957)

Table 6. Irrigation Water quality classification based on IRWQI value

Range of values	Category	Ground water locations
<50	Excellent water	1-3, 5-7, 18, 21, 23-25, 33, 35-38, 40, 41, 43-45, 47, 53, 54, 58, 63
50-100	Good water	4, 8-17, 20, 22, 26-32, 34, 39, 42, 46, 48-52, 55-57, 59-62, 64, 66
100-200	Poor water	---
200-300	Very poor water	---
>300	Unsuitable	19, 31

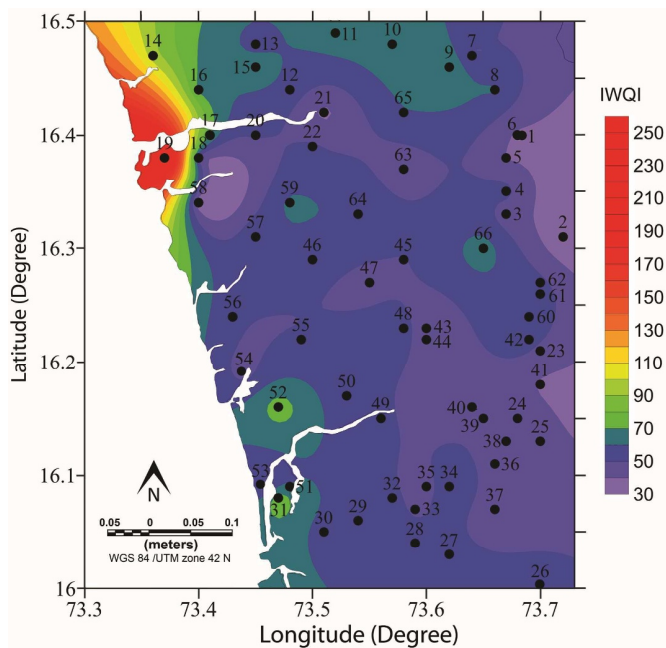


Fig.15. Spatial distribution map of irrigation water quality index.

weighted irrigation water quality index (IWQI) was calculated using the relationship (Brown et al., 1972).

$$IWQI = \sum(W_n * Q_n) \quad (10)$$

Where W_n = unit weight of the n^{th} parameter, Q_n = sub-index of the corresponding parameter.

The unit weights and sub-index of all the parameters computed and used are summarized in Table 5. The results of IWQI are particularized in Table 6. As indicated in this table, most of the groundwater samples are excellent to good category. However, samples 19 and 31 reveal IWQI values greater than 300, which is above the permissible limit and thus unsuitable for irrigation. The suitability of groundwater for irrigation in the study area is shown in Fig. (15). Groundwater quality is fairly suitable in most of the parts, except at two locations which are unsuitable.

CONCLUSIONS

The hydrochemical analysis of the groundwater samples in parts of northern Sindhudurg district reveals alkaline condition at most of the sampling points and the physico-chemical parameters signify that groundwater quality is good and are within permissible limits prescribed by the World Health Organization, except at a few coastal stations. The groundwater of the area is characterized by Ca^+ - Mg^{2+} - HCO_3^- , Ca^+ - Mg^{2+} - Cl^- and Na^+ - Cl^- facies as indicated in both piper trilinear diagram and Chadha's plot. Gibb's diagram suggests that all the water samples fall predominantly in the rock dominance, whereas two samples (19 and 31) fall in evaporation dominance due to the effect of saline water. The EC and TDS values at these locations are brackish (3.33%), presumably due to saline water ingress, however, groundwater at the majority (96.67%) of locations are within the permissible limits and thus freshwater type. Likewise, the molar ratio of $\text{Cl}^-/\text{HCO}_3^-$ vs. Cl^- suggests that only two samples are strongly affected by seawater intrusion, as these wells (19 and 31) are located near the backwaters and fall in the vicinity of Arabian Sea. Furthermore, the ionic ratios of $\text{Mg}^{2+}/\text{Na}^+$ vs $\text{Ca}^{2+}/\text{Na}^+ < 1$ and $(\text{Na}^+/\text{Cl}^-)$ vs EC also reveals the ion exchange in association with mineral dissolution and water-rock interaction (silicate weathering) processes playing a vital role in the study area. This is also validated through PCA of geochemical parameters suggesting that the first

three principal components accounting for 92% of the cumulative variation.

The suitability of groundwater for irrigation was evaluated based on SAR, %Na, RSC, MAR and KR. The SAR values suggest that most of the samples fall in the excellent category except two (wells 19 and 31), where the SAR values are 73.6 and 31.2 respectively. Similar results are observed from the USSL diagram which suggests that the majority of the groundwater samples fall under low salinity to low sodium type water (C1-S1 category), and very few samples represent medium salinity to low sodium type C2-S1. Only one sample fall under high salinity to low sodium type C3-S1, while two samples fall in very high salinity to very high sodium type of water which are unfit for irrigation. The permeability index suggests that about 80% of the samples fall in 25% of maximum permeability, signifying the fact that the soil permeability is affected by long term use of water containing salts like sodium, calcium, magnesium and bicarbonate for irrigation.

From the foregoing, it is revealed that the drinking water quality index is 96% in the study area and thus falls under the 'excellent' to 'good' category. Nearly 4% of the coastal samples reveal 'poor to unsuitable' quality, where the EC and other major ions have exceeded their permissible limit thereby making the water unfit for drinking. Suitability of irrigation water quality index indicates that most of the water is of excellent to good quality for irrigation, except for a few coastal samples. The present study signifies that hydrogeological processes like rock-water interaction, ion exchange and seawater intrusion along the coast are the chief controlling factors for the groundwater chemistry, and thus regular monitoring and assessment of the groundwater quality is essential.

Acknowledgements: The authors are indebted to Dr. D.S. Ramesh, Director, Indian Institute of Geomagnetism, New Panvel for the motivation and consent to publish the work. The authors express their gratitude to Shri B.I. Panchal for drafting the figures.

References

- APHA (American Public Health Association), (2012) Standard methods for the examination of water and waste water. 21st edn. American Public Health Association, Washington, DC.
- Brown, R.M., McClelland, N.J., Deiniger, R.A., O'Connor, M.F.A. (1972) Water quality index-crossing the physical barrier. In: Jenkis SH (ed) Proceedings in International Conference on Water Pollution Research, Jerusalem, 787-797.
- Bureau of Indian Standards (BIS) (2012) Indian standard drinking water specifications. (2nd Revision) BIS 10500: 2012, New Delhi.
- Chadha, D.K. (1999) A proposed new diagram for geochemical classification of natural waters and interpretation of chemical data. Hydrogeol. Jour., v.7(5), pp. 431-439.
- Chatterjee, C. and Razuddin, M. (2002) Determination of Water Quality Index (W.Q.I.) of a degraded river in Asanil Industrial area, Ranigunj, Burdwan, West Bengal. Nature Environ. Poll. Technology, v.1(2), pp.181-189.
- Central Groundwater Board (CGWB) (2014) Groundwater information, Sindhudurg district, Maharashtra. Technical Report 1835/DB/2014.
- Deshpande, G.G. (1998) Geology of Maharashtra. Geological Society of India, Bangalore, 223p.
- Dikshit, K.R. (2001) Drainage basins of Konkan: Forms and characteristics. Mem. Geol. Soc. India, v.47, pp.307-325.
- Domenico, P.A., Schwartz, F.W. (1990) Physical and Chemical Hydrogeology. Wiley, New York, NY, USA.
- Doneen, L.D. (1964) Water quality for agriculture. Department of irrigation, University of California, Davis, p.4.
- Eaton, E.M. (1950) Significance of carbonates in irrigation waters. Soil Sci. v.69, pp.123-133.
- Freeze, R.A. and Cherry, J.A. (1979) Groundwater: Englewood Cliffs, NJ, Prentice-Hall, 604p.
- Garg, V.K., Suthar, S., Singh, S., Sheoran, A., Nagpal, G., Meenakshi and Jain, S. (2009) Drinking water quality in villages of southwestern Haryana,

- India: assessing human health risks associated with hydrochemistry. *Environ. Geol.*, v.58(6), pp.1329-1340.
- Gibbs, R.J. (1970) Mechanisms controlling worlds water chemistry. *Science*, v.170, pp.1088-1090.
- Hem, J.D. (1991) Study and Interpretation of Chemical Characteristics of Natural Water. U. S. Geol. Surv. Water Supply Paper No.2254.
- Hamill, L. and Bell, F.G. (1986) G.W. Resource and Development, Butter Worths London, 344p.
- Hounslow, A.W. (1995) Water quality data: analysis and interpretation. Lewis Pub., New York.
- Kalpana, L. and Elango, L. (2013) Assessment of groundwater quality for drinking and irrigation purposes in Pambar river sub-basin, Tamil Nadu. *Indian Jour. Environ. Prot.*, v.33(1), pp.1-8.
- Kelly, W.P. (1957) Adsorbed sodium cation exchange capacity and percentage sodium sorption in alkali soils. *Science*, v.84, pp.473-477.
- Kovalevsky, V.S., Kruseman, G.P. and Rushton, K.R. (2004) Groundwater studies: an international guide for hydrogeological investigations. United Nations Educational, Scientific and Cultural Organization, Paris.
- Kumar, M., Kumari, K., Ramanathan, A.L. and Saxena, R. (2007) A comparative evaluation of groundwater suitability for irrigation and drinking purposes in two intensively cultivated districts of Punjab, India. *Environ. Geol.*, v.53(3), pp.553-574.
- Kumaran, K.P.N., Shindikar, M. and Limaye, R. (2004) Mangrove associated lignite beds of Malvan, Konkan: evidence for higher sea-level during the Late Tertiary (Neogene) along the west coast of India. *Curr. Sci.*, v.86, pp.335-340.
- Kumar, S., Singh, R., Venkatesh, A.S. et al., 2019. Medical Geological assessment of fluoride contaminated groundwater in parts of Indo-Gangetic Alluvial plains. *Sci Rep* 9-16243. doi: 10.1038/s41598-019-52812-3.
- Kumar, S., Venkatesh, A.S., Singh, R., Udaybhanu, G., Saha, D., 2018. Geochemical signatures and isotopic systematics constraining dynamics of fluoride contamination in groundwater across Jamui District, Indo-Gangetic alluvial plains, India. *Chemosphere*. doi: 10.1016/j.chemosphere.2018.04.116.
- Li, P., Wu, J. and Qian, H. (2013) Assessment of groundwater quality for irrigation purposes and identification of hydrogeochemical evolution mechanisms in Pengyang County, China. *Environ. Earth Sci.*, v.69(7), pp.2211-2225.
- Maiti, S., Gupta, G., Erram, V.C. and Tiwari, R.K. (2012) Delineation of shallow resistivity structure around Malvan, Konkan region, Maharashtra by neural network inversion using vertical electrical sounding measurements. *Environ. Earth Sci.* doi: 10.1007/s12665-012-1779-8.
- Milovanovic, M. (2007) Water quality assessment and determination of pollution sources along the Axios / Vardar River, Southeast Europe. *Desalination*, v.213, pp.159-173.
- Naladala, N.R., Singh, R., Katiyar, K.L.D., Bose, P., Dutta, V. (2018) Effect of Pre-Ozonation on Haloacetic Acids Formation in Ganga River Water at Kanpur, India. *J. Institute Engineers India Series-A* 99:37. doi:10.1007/s40030-017-0226-y.
- Naladala, N.R., Singh, R., Venkatesh A.S., Bose, P., Babu K.P. and Narayan, I. D. (2020) Effectiveness of Bio-Activated Carbon Filtration and Ozonation on Control of Halo Acetic Acids Formation during Chlorination of Ganga River Water at Kanpur, India. *Ozone: Science & Engineering*, 42:1, 24-35, doi: 10.1080/01919512.2019.1604205
- Paliwal, K.V. (1972) Irrigation with Saline Water. Water Technology Centre, Indian Agriculture Research Institute, New Delhi, 198p.
- Paranjpe, S.C. (2007) Development and augmentation of groundwater resources with emphasis on deep aquifers, Pune metropolitan region, Maharashtra. Unpublished Ph.D. thesis, University of Pune, India, 186p.
- Piper, A.M. (1953) A graphical procedure in the geochemical interpretation of water analysis. *Trans. Am. Geophys. Union*, v.25, pp.914-928.
- Ramesh, K. and Elango, L. (2011) Groundwater quality and its suitability for domestic and agricultural use in Tondiar river basin, Tamil Nadu, India. *Environ. Monit. Assess.*, doi: 10.1007/s10661-011-2231-3.
- Ravikumar, P., Somashekar, R.K. and Angami, M. (2010) Hydrochemistry and evaluation of groundwater suitability for irrigation and drinking purposes in the Markandeya River basin, Belgaum District, Karnataka State, India. *Environ. Monit. Assess.*, v.173(1-4), pp.459-487.
- Richards, L.A. (1954) Diagnosis and improvement of saline and alkaline soils. Department of Agriculture Hand Book, US, 60p.
- Rivers, C.N., Hiscock, K.M., Feast, N.A., Barrett, M.H. and Dennis, P.F. (1996) Use of nitrogen isotopes to identify nitrogen contamination of the Sherwood sandstone aquifer beneath the city of Nottingham, UK. *Hydrol. J.*, v.4(1), pp.90-102.
- Singh, A.K., Mondal, G.C., Singh, T.B., Singh, S., Tewary, B.K. and Sinha, A. (2012) Hydrogeochemical processes and quality assessment of groundwater in Dumka and Jamtara districts, Jharkhand, India. *Environ. Earth Sci.*, v.67(8), pp.2175-2191.
- Singh, A.K., Raj, B., Tiwari, A.K. and Mahato, M.K. (2013) Evaluation of hydrogeochemical processes and groundwater quality in the Jhansi district of Bundelkhand region, India. *Environ. Earth Sci.*, v.70(3), pp.1225-1247.
- Singh, R., Syed, T.H., Kumar, S., Kumar, M. and Venkatesh, A.S. (2017a) Hydrogeochemical assessment of surface and groundwater resources of Korba coalfield, Central India: environmental implications. *Arab Jour. Geosci.*, v.10, pp.318, doi:10.1007/s12517-017-3098-6.
- Singh, R., Venkatesh, A.S., Syed, T.H., Reddy, A.G.S., Kumar, M. and Kurakalva, R.M. (2017b) Assessment of potentially toxic trace elements contamination in groundwater resources of the coal mining Area of the Korba coalfield, Central India. *Environ. Earth Sci.*, doi:10.1007/s12665-017-6899-8.
- Singh, R., Venkatesh, A.S., Syed, T.H., Surinaidu, L., Pasupuleti, S., Rai, S.P. and Kumar, M. (2018) Stable isotope systematics and geochemical signatures constraining groundwater hydraulics in the mining environment of the Korba Coalfield, Central India. *Environ. Earth Sci.*, v.77, pp.548, doi:10.1007/s12665-018-7725-7.
- Singha, S., Pasupuleti, S., Durbha, K.S., Singha, S.S., Singh, R., Venkatesh, A.S. (2019) An analytical hierarchy process-based geospatial modeling for delineation of potential anthropogenic contamination zones of groundwater from Arang block of Raipur district, Chhattisgarh, Central India. *Environ. Earth Sci.*, v.78, pp.694, doi: 10.1007/s12665-019-8724-z.
- Singha, S.S., Pasupuleti, S., Singha, S., Singh, R. and Venkatesh, A.S. (2019) Analytic Network Process based approach for delineation of groundwater potential zones in Korba district, Central India using remote sensing and GIS. *Geocarto Internat.*, pp.1-23, doi: 10.1080/10106049.2019.1648566.
- Stumm, W. and Morgan, J.J. (1996) Aquatic Chemistry. Wiley, New York, 1022p.
- Subba Rao, N. and Krishna Rao, G. (1991) Groundwater quality in Visakhapatnam urban area, Andhra Pradesh. *Indian J. Environ. Health*, v.33(1), pp.25-30.
- Sundar, M.L. and Saseetharan, M.K. (2008) Ground water quality in Coimbatore, Tamil Nadu along Noyyal River. *Jour. Environ. Sci. Engg.*, v.50, pp.187-190.
- Szabolcs, I. and Darab, C. (1964) The Influence of Irrigation Water of High Sodium Carbonate Content of Soils. *In: Proc. 8th International Congress of ISSS*, v.2, pp.803-812.
- Todd, D.K. (1980) Groundwater hydrology. 2ndedn. Wiley, New York, 535p.
- USDA (1954) Diagnosis and improvement of saline and alkali soils. U.S. Agric. Handbook No.60. U.S. Dept. Agric., Washington D.C.
- USSL (1954) Diagnosis and improvement of saline and alkali soils, United States Department of Agriculture, Agricultural handbook No.60, Washington, D.C, 147p.
- Werner, A.D. and Simmons, C.T. (2008) Impact of sea-level rise on sea water intrusion in coastal aquifers. *Ground Water*, v.47(2), pp.197-204.
- WHO (2011) WHO guidelines for drinking water quality. 4th edn. World Health Organization, Geneva, pp.1-564.
- Wilcox, L.V. (1955) Classification and use of irrigation waters. USDA, Washington, DC.
- Xue, Y., Xie, C. and Wu, J. (1999) Seawater intrusion and research on movement of interface of fresh-saline water, Nanjing, China. Nanjing University Press.

(Received: 21 February 2020; Revised form accepted: 8 September 2020)